Available online at www.sciencedirect.com
SCIENCE DIRECT
Sensors and Actuators A 128 (2006) 278–289
SENSORS AND ACTUATORS A PHYSICAL
www.elsevier.com/locate/sna

The structure optimization of the carbon nanotube film cathode in the application of gas sensor

Zhang Yong [a,*], Liu Junhua [a], Li Xin [b], Zhu Changchun [b]

[a] *Department of Electrical Engineering, Xi'an Jiaotong University, Xi'an, Shaanxi 710049, China*
[b] *Vacuum Micro-Electronic & Micro-Electronic Mechanical Institute, Department of Electronic and Information Engineering, Xi'an Jiaotong University, Xi'an, Shaanxi 710049, China*

Received 21 July 2005; received in revised form 2 January 2006; accepted 19 January 2006
Available online 28 February 2006

Abstract

The carbon nanotube (CNT) film is used to fabricate the novel carbon nanotube film cathode (CNTFC) gas sensor, and the working voltage of the novel sensor at atmospheric pressure decreases to several hundred volts from the value of more than thousand volts of the traditional discharge gas sensor, however it is limited by that the space charge in the gap is very hard to diffuse after the breakdown of the gap. This makes the gap in conductance and next self-sustaining dark discharge impossible. To solve the problem, experimental study and simulation calculation were conducted to optimise the structure of CNTFC. Five CNTFCs with different structures were designed and the experiments were conducted to study discharge principle. It shows that the CNTFC could be chosen as a gas sensor, when it has the three characteristics of low working voltage, working at self-sustaining dark discharge state, and the space charge in the gap being easy to diffuse. The electric field distributions of the five CNTFCs were studied and calculated by using the finite element method. The results of the simulations and the experiments show that it is reasonable to use the CNTFC with the above three characteristics as a novel gas sensor.

Keywords: Carbon nanotube; Sensor; Gas discharge; Structure optimization; Electric field

1. Introduction

Gas sensors operate by a variety of fundamentally different mechanisms [1–9], and there are generally two kinds [10,11] of gas sensors: one kind is based on the chemical mechanism and the physical mechanism [12–23], the other on the physical mechanism [24,25]. Among all gas sensors, ionization gas sensors are mainly used as the gas detector in advanced gas analyzer such as chromatograph and mass spectrograph to realize the high-precision measurement of gas concentration after the gas mixture is separated. However, the traditional ionization sensors are limited by high working voltage, high vacuum environment, and their huge and bulky architecture.

The novel MEMS ionization micro-sensor [26] (reported in 1998) with the gap distance 50 μm decreased the breakdown voltage of several gases from the value of more than thousand volts of the traditional discharge gas sensor to the range of 350–550 V at atmospheric pressure. However, because the single tip with the curvature radius of micrometer order was used as the cathode, the electric field distribution was very nonuniform and the corona discharge at high voltage was very easy to occur. Later, when it was used to take place of flammable ionization detector (FID) of chromatograph used in National Weather Bureau of Japan and measure the trace SO_2 in the atmosphere, it worked at corona discharge state and its working voltage increased up to 2000 V in condition of the gap distance 50 μm.

The novel carbon nanotube film cathode (CNTFC) gas sensor with CNT array film as the cathode [27] (reported in 2001), worked at self-sustaining dark discharge state and the breakdown voltage is low. In condition of the gap distance 91 μm of the CNTFC, the breakdown voltages of several gases decreased to less than 220 V at atmospheric pressure and room temperature. After the breakdown of the gap occurred, the large quantity of space charge existed in the gap, and the space charge in the gap made the insulation resistance between cathode and anode decreasing from the infinite to the finite. It was very difficult to clear the space charge in the gap at atmospheric pressure except

* Corresponding author. Tel.: +81 080 5384 1998; fax: +81 045 566 1487.
E-mail address: zhy-lemon@sohu.com (Y. Zhang).

0924-4247/$ – see front matter © 2006 Elsevier B.V. All rights reserved.
doi:10.1016/j.sna.2006.01.027

taking apart CNTFC, cleaning the anode plate and fabricating CNTFC again. Thus, the next self-sustaining dark discharge experiment could not be conducted if the space charge was not cleared out of the gap.

The carbon nanotube film anode (CNTFA) gas sensor with CNT array film as the anode [28] (reported in 2003), worked at corona discharge state, and could be used to identify several single gases through the measured breakdown voltages. However, CNTFA worked at vacuum environment and thus needed huge vacuum system. What was proposed and conducted in the end was to combine the CNTFA with chromatograph.

Among the three novel discharge gas sensors, CNTFC gas sensor is superior to the other two sensors in such characteristics as working at atmospheric pressure, self-sustaining dark discharge and low working voltage. To solve the problem of difficult diffusion of the space charge in the gap after the breakdown and make the continuous measurement possible, the structure optimization of CNTFC is studied.

2. Establishment of the gas mixing system and the test set-up

To study the discharge principle of the CNTFC in the gas, a gas mixing system and the test set-up were established. The gas mixing system was used to offer the gas mixture in a controlled flux and in an environment gas—N_2, and the test set-up was used to measure the discharge *I–V* characteristic of the CNTFC.

2.1. The gas mixing system

A gas mixing system (Fig. 1a) in a controlled flux and in an environment gas was established to obtain the gas mixture with different concentrations. There are four high-pressure gas bottles G1–G4. G1, G2, and G3 supply the measured gases, and G4 supplies the environment gas. DV1–DV4 are four pressure-control valves, and HV1–HV4 are four shut-off valves. MFC1–MFC4 are four mass flux meters, and could continuously control the gas flux f_1–f_4. The pressure of the high-pressure bottle could be decreased to 1–2 atm through the pressure-control valves, and the pressure P_s at the outlet of the mass control meters is decreased to 1 atm, as same as the pressure P_g in the measuring chamber. The single gas pressure P, with the unit of Pa is as the following:

$$P_i = \frac{P_s f_i}{\sum_{i=1}^{n} f_i} \tag{1}$$

The quantity in mol $\varphi(i)$ of the ith single gas is as the following:

$$\varphi(i) = \left(\frac{P_s}{P_g}\right)\left(\frac{f_i}{\sum_{i=1}^{n} f_i}\right) \tag{2}$$

Because $P_s = P_g$, the formula (2) can be expressed as the following:

$$\varphi(i) = \frac{f_i}{\sum_{i=1}^{n} f_i} \tag{3}$$

where n is the number of the components in the gas mixture including the environment gas. Different concentrations of single gases CH_4 and CO in N_2 and the two-gas mixture CH_4–CO in N_2 could be obtained through controlling the flux of CH_4, CO, and N_2. For example: (1) when the single gas of CH_4 is mixed with the environment gas N_2, $n = 2$; the flux of CH_4 and N_2 are controlled to obtain different concentration of CH_4. (2) When the single gas of CO is mixed with the environment gas N_2, $n = 2$; the flux of CO and N_2 are controlled to obtain different concentration of CO. (3) When the two-gas mixture of CH_4–CO is mixed with N_2, $n = 3$; the flux of CH_4, CO, and N_2 are controlled to obtain different concentration of CH_4–CO mixture.

Because the four flux meters have the same accuracy of ±2%, the concentration deflections of the single gas and the two-gas mixture are calculated according to the formulas of (4) and (5):

$$\gamma_{\varphi(1)} = \left(\frac{f_4}{f_1 + f_4}\right)(\gamma_{f_1} - \gamma_{f_4}) \tag{4}$$

$$\gamma_{\varphi(2)} = \frac{f_3 + f_4}{f_2 + f_3 + f_4}\gamma_{f_2} - \frac{f_3}{f_2 + f_3 + f_4}\gamma_{f_3} - \frac{f_4}{f_2 + f_3 + f_4}\gamma_{f_4} \tag{5}$$

where $\gamma_{f_1}, \gamma_{f_2}, \gamma_{f_3}$, and γ_{f_4} are the accuracy of the four flux meters, $\gamma_{\varphi(1)}$ is the accuracy of the concentration of the single gas, and $\gamma_{\varphi(2)}$ is the accuracy of the concentration of the two gas mixture, $\gamma_{\varphi(1)}$ and $\gamma_{\varphi(2)}$ are calculated according to the formula (4) and (5), respectively, and are all ±4%. Thus, when

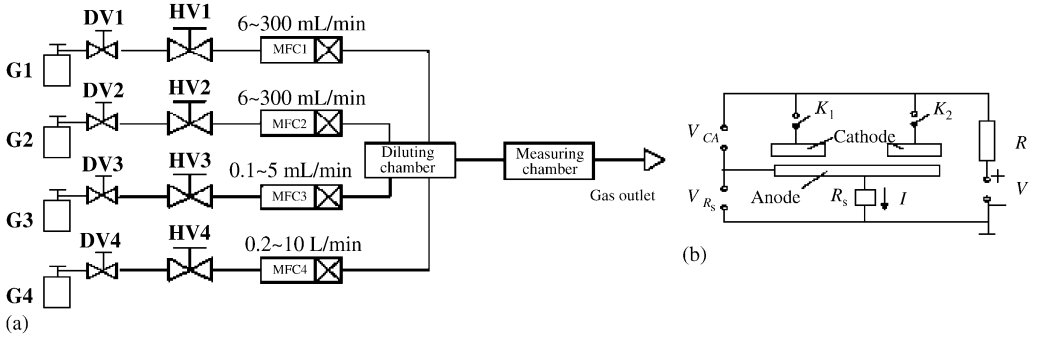

Fig. 1. The experiment set-up. (a) Gas mixing system; (b) the test set-up of the discharge *I–V* characteristic of the CNTFC.

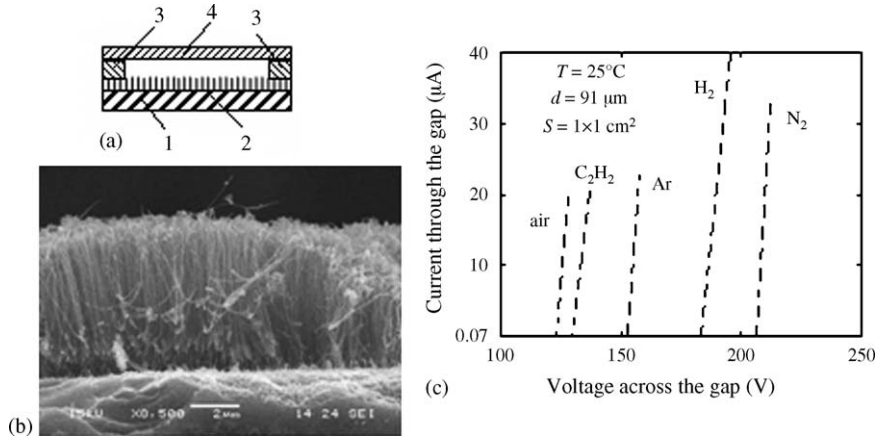

Fig. 2. The CNTFC gas sensor fabricated in reference [27]. (a) The structure of the CNTFC gas sensor (1, silicon slice cathode; 2, CNTFC; 3, insulator strip of mica; 4, ITO film conductance glass anode); (b) carbon nanotubes array; (c) the discharge *I–V* characteristics of the CNTFC gas sensor in several single gases (air, C_2H_2, Ar, H_2, and N_2), at room temperature and the atmospheric pressure.

the measuring concentration of CO is 500×10^{-6} L/L, there is the maximum concentration deflection of $\pm 20 \times 10^{-6}$ L/L, less than the measuring accuracy requirement of CO concentration ±5%. When the measuring concentration of CH_4 is $40{,}000 \times 10^{-6}$ L/L, there is the maximum concentration deflection of $\pm 1600 \times 10^{-6}$ L/L, less than the measuring deflection requirement $\pm 3000 \times 10^{-6}$ L/L of CH_4. It shows that the gas mixing system meets the measuring requirements of CH_4 and CO.

2.2. The test set-up of discharge I–V characteristic of CNTFC

The test set-up (Fig. 1b) measuring the discharge *I–V* characteristic of CNTFC is composed of several parts as the following:

(1) Two-sensor array.
(2) The current-limiting resistance R (2.1 MΩ).
(3) The sampling resistance R_s (10 kΩ).
(4) DC standard high-voltage generator (NJ1, 1.5 kV), supplying CNTFC DC high-voltage V in the range of 0–1.5 kV.
(5) Keithley digital multi-meter (with the resolution of 10 nV), measuring the voltage V_{R_s} of R_s to obtain the discharge current I.

The CNTFC is placed in a measuring chamber with electrical feed-through, and the environment pressure is atmospheric pressure.

3. CNTFC gas sensor fabricated in reference [27]

It was supposed in reference [27] that CNT array film was used as the cathode, and a novel gas sensor with the CNT film cathode (CNTFC) was fabricated to identify the gas variety. The sensor works at self-sustaining dark discharge, which is different with the corona discharge and the glow discharge. Because the CNT film was used as the cathode, and the tip of nanotube supplies very high electric field intensity, the breakdown voltage decreases from thousand volts of the traditional discharge gas sensor to less than 220 V with the gap distance 91 μm.

3.1. The characteristics and the structure of CNTFC gas sensor

The structure of the sensor is shown in Fig. 2a. The CNT film was grown by thermal chemical vapor deposition (TCVD) [29,30] on Si (silicon) substrate. Nanotubes in the film (Fig. 2b) are ~50 nm in diameter, ~4 μm long, with ~50 nm separation between nanotubes.

3.2. I–V characteristics of CNTFC gas sensor

The CNTFC gas sensor in Fig. 2a with the gap distance 91 μm and the CNT film area of 1 cm × 1 cm (1 cm^2) is used to conduct the experiment. *I–V* characteristics of the self-sustaining discharge of five single gases are obtained, shown in Fig. 2c. The breakdown voltages of five single gases are less than 220 V and lower than those of the novel MEMS gas sensor [26], 350–550 V. The currents at the breakdown increase to microampere order, three orders larger than nanoampere order of those of the novel MEMS gas sensor [26]. The breakdown voltages and the currents at breakdown are shown in Table 1. We can see that different kinds of gases have different breakdown voltages and the currents at breakdown. It shows that different kinds of gases have different conductance. Thus, a novel gas sensor can be fabri-

Table 1
Breakdown voltages and currents at breakdown of #1 CNTFC electrode in five pure gases

Gas	Breakdown voltage (V)	Current at breakdown (pA)
Air	128	20.0
C_2H_2	137	20.8
Ar	158	23.0
H_2	196	40.0
N_2	212	33.0

cated with CNT film as the cathode, and the gas variety can be identified using the breakdown voltage. For example:

(1) When the breakdown voltage of the CNTFC in a measured single gas is 128 V, it can be concluded that the measured single gas is air.
(2) When the breakdown voltage of the CNTFC in a measured single gas is 137 V, it can be concluded that the measured single gas is C_2H_2.
(3) When the breakdown voltage of the CNTFC in a measured single gas is 158 V, it can be concluded that the measured single gas is Ar.
(4) When the breakdown voltage of the CNTFC in a measured single gas is 196 V, it can be concluded that the measured single gas is H_2.
(5) When the breakdown voltage of the CNTFC in a measured single gas is 212 V, it can be concluded that the measured single gas is N_2.

3.3. Problem of CNTFC gas sensor fabricated in reference [27]

In the experiment of studying the breakdown voltage-gas concentration relationship using the CNTFC reported in reference [27], the anode and cathode plates were of 1 cm length, 1 cm width, and 0.05 cm thick. And it was found that after the breakdown of the gap occurred, it was very hard to clear out the space charge in the gap, when the voltage V across the gap decreased to 0 V and the gap was blown by using an ear-washing ball in a given flux of air. Thus, the next discharge experiment could not be conducted until the CNTFC was taken apart and then assembled together again. The experiments show that the area of the CNTFC with 1 cm length and 1 cm width is relatively large, and is not favourable for the space charge in the gap to diffuse. Thus, the area of the CNTFC is required to decrease. However, if the area of the cathode is too small, the distribution of the electric field in the gap will be very nonuniform and the corona discharge at higher voltage will be easy to occur. If the area of the cathode is too large, the distribution of the electric field in the gap will be relatively uniform and the self-sustaining dark discharge will occur. However, the quantity of the space charge after the breakdown of the gap will be large and will be not favourable for the space charge in the gap to diffuse. So, to keep the CNTFC working at the self-sustaining dark discharge state, how much should the area of the CNTFC decrease to? It is required to study the optimization of the CNTFC structure, and the experiments and the simulations on the optimization are conducted in the following.

4. Experiment study of CNTFC structure optimization

In the experiment study of CNTFC structure optimization, five different CNTFC structures are designed, and the experiments are conducted to study their discharge principle. The CNTFCs used in the electrodes are the CNT films grown by TCVD on Si substrates with different sizes.

4.1. Design and study of #1 CNTFC electrode with plate-plate structure

4.1.1. Design of #1 CNTFC electrode with plate-plate structure

#1 Plate-plate structure electrode (Fig. 2a) is the initial design, reported in reference [27]. The effective face-to-face area between the cathode and the anode is 1 cm × 1 cm (1 cm^2), and the insulator between the cathode and the anode uses the mica piece. The anode is composed of ITO (In/SnO_2) film glass plate with ITO film electrically conductive, and is convenient to observe whether there are the light phenomena during the discharge.

4.1.2. Experimental study of discharge principle of #1 CNTFC electrode

#1 Plate-plate structure electrode with the gap distance 91 μm is used to conduct the experiments and study I–V characteristics (Fig. 2c) of five single gases (air, Ar, N_2, H_2, and C_2H_2) at 100% concentration, room temperature, and atmospheric pressure. Usually, the gas at atmospheric pressure will not have the conductance until the voltage increases to more than thousands volts. However, the breakdown voltages in Fig. 2c are less than 220 V, decreasing several tens folds, and the currents at breakdown are 20–40 μA. Then, #1 plate-plate structure electrode with the gap distance 170 μm is used to conduct the experiments and study I–V characteristic of air, the breakdown voltage is 330 V and the current at breakdown is 84.6 μA. In comparison with the breakdown voltage of 125 V with the gap distance 91 μm, the breakdown voltage of air increases when the gap distance increases, and the comparison is shown in Table 2. There are no light phenomena during the discharge, thus the discharge is self-sustaining dark discharge. The breakdown voltage of #1 electrode is low, and those in the above experimental data do not exceed 330 V. However, the space charge in the gap is very hard to diffuse after the breakdown of the gap.

4.2. Design and study of #2 CNTFC electrode with strip-plate (with small holes) structure

4.2.1. Design of #2 CNTFC electrode with strip-plate (with small holes) structure

The structure of #2 electrode is shown in Fig. 3a–c, the cathode is composed of the CNT film and the ITO film glass plate, and the anode is composed of the ITO film glass plate. The CNT film is grown by TCVD on a Si substrate with 2.0 mm width, 40 mm length and 0.5 mm thick, and is stuck to the ITO film glass plate with the electric conductance glue. In comparison with #1 electrode, #2 electrode decreases the width of CNT

Table 2
The breakdown characteristics of #1 electrode with the gap distances of 91 μm and 170 μm in air

Gap distance (μm)	Breakdown voltage (V)	Current at breakdown (μA)
91	125	20.0
170	330	84.6

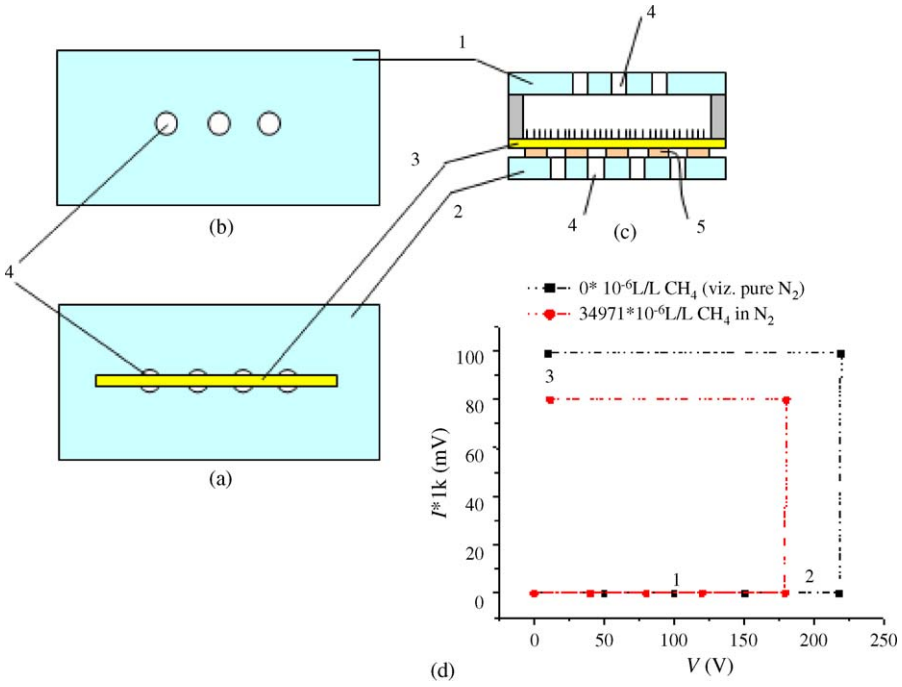

Fig. 3. #2 CNTFC strip-plate electrode with small holes. (a) Cathode: ITO film conductance glass plate with the CNT film stuck on; (b) anode: ITO film conductance glass plate; (c) the CNTFC electrode; (d) the discharge *I–V* characteristics of #2 electrode in CH_4–N_2 mixture (at CH_4 concentrations 0×10^{-6} L/L (viz. pure N_2) and 34,971 $\times 10^{-6}$ L/L), at room temperature and atmospheric pressure (1, ITO film conductance glass anode; 2, ITO film conductance glass cathode; 3, CNTFC; 4, the ventilating holes; 5, the electric conductance glue).

film. The polyester film with 100–200 μm thick is used as the insulator between the cathode and the anode of #2 electrode. There are even-separation aligned ventilating holes with 4 mm diameter and 3 mm separation between holes, convenient for the space charge to diffuse. The ventilating holes are eroded according to the following steps: (1) olefin is used as the cover film on the ITO film glass plate except the area of holes; (2) and then HF acid is used to erode the holes. The areas of two ITO film glass plates are all 4 cm × 8 cm (32 cm^2), with the effective face-to-face area between the CNT film and the anode 2 × 0.2 cm × 0.3 cm (0.12 cm^2), decreasing one order in comparison with 1 cm × 1 cm (1 cm^2) of #1 electrode.

4.2.2. Experimental study of discharge principle of #2 CNTFC electrode

#2 CNTFC electrode with strip-plate (with small holes) structure with the gap distance 170 μm is used to conduct the experiments and study *I–V* characteristics (Fig. 3d) of CH_4 mixed with N_2 at the concentrations of CH_4 0×10^{-6} L/L (viz. pure N_2) and 34,971 $\times 10^{-6}$ L/L, room temperature and atmospheric pressure. The working point 2 in Fig. 3d shows that N_2 and CH_4–N_2 mixture are already in the state of the self-sustaining dark discharge, and the current across the gap increases rapidly. The working point 3 shows that pure N_2 and CH_4–N_2 mixture are already in the state of stable discharge with no light phenomenon after the self-sustaining dark discharge. Here, the current across the gap keeps constant, the large quantity of space charge appears in the gap, and the resistance of the gap decreases from the infinite to the finite. The space charge in the gap or the constant current across the gap (viz. the current at breakdown) at the working point 3 makes the voltage across the gap at the working point 3 lower than that at the working point 2. The phenomena can be explained by Rogowski Space Charge Theory.

The breakdown voltage of #2 electrode is low, and those in Fig. 3d are 80 V and 100 V, respectively. The space charge in the gap of #2 electrode is easy to diffuse because of the ventilating holes in the anode and cathode plates.

4.3. Design and study of #3 CNTFC electrode with strip-plate (with large holes) structure

4.3.1. Design of #3 CNTFC electrode with strip-plate (with large holes) structure

#3 Electrode structure (Fig. 4a and b) is also the strip-plate structure, and the metal plate with large ventilating holes is used to replace the ITO film glass plates with small ventilating holes of #2 electrode. The CNT film is stuck to the metal plate cathode with the area of 2 cm × 7.7 cm (15.4 cm^2) (almost half of that of #2 electrode 4 cm × 8 cm (32 cm^2)), using the electric conductance glue. The holes in the cathode plate are 8 mm in diameter and 1.5 mm in separation between holes, and the holes in the anode 10 mm and 3 mm, respectively. The effective face-to-face area between the CNT film and the anode is 2 × 0.2 cm × 0.3 cm (0.12 cm^2), and the polyester film is used as the insulator between the cathode and the anode.

4.3.2. Experimental study of discharge principle of #3 CNTFC electrode

#3 Electrode with strip-plate structure with large holes is used to conduct the experiments and study *I–V* characteristics

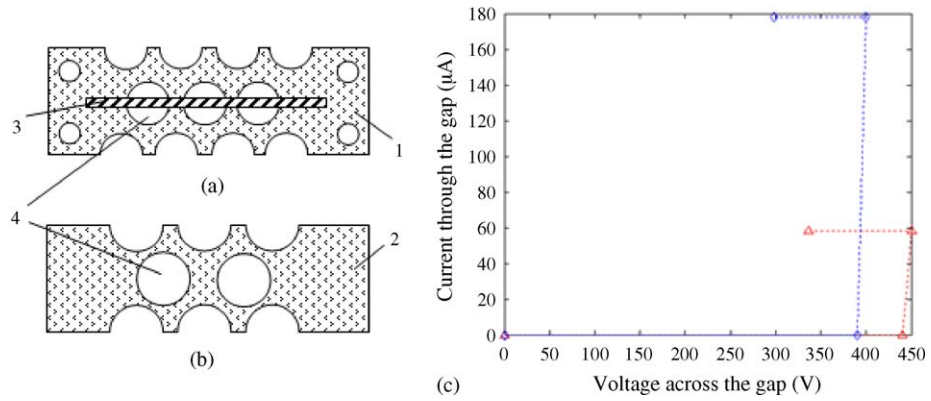

Fig. 4. #3 CNTFC strip-plate electrode with large holes. (a) Cathode: brass cathode plate (the ventilating holes with 8 mm diameter and 1.5 mm separation between holes) and the CNT film stuck on brass cathode plate; (b) anode: brass anode plate (the ventilating holes with 10 mm diameter and 3 mm separation between holes); (1, brass cathode plate; 2, brass anode plate; 3, the CNT film cathode; 4, the ventilating holes); (c) The discharge *I–V* characteristics of #3 CNTFC electrode in air.

(Fig. 4c) of air and the gap distance is 170 μm. The corona discharge occurred and there was the light phenomenon near the cathode. The corona discharge voltages of #3 electrode in air are 390 V and 440 V, respectively, and the currents at the corona discharge are relatively high, 60 μA and 180 μA, respectively. However, the breakdown voltages of #1 and #2 electrodes with the same gap distance in the air, 330 V and 90 V, are all less than those of #3 electrode. When there is the constant current across the gap, the resistance of the gap decreases from the infinite to the finite, and the voltage across the gap decreases from the initial value to the value less than the initial. The initial voltage across the gap is the voltage supplied by DC standard high-voltage generator. It shows that because the diameter of the ventilating holes increases, the nonuniformity of the electric field distribution increases, and thus the corona discharge occurs in the gap.

4.4. Design and study of #4 CNTFC electrode with tip-plate structure

4.4.1. Design of #4 CNTFC electrode with tip-plate structure

#4 CNTFC electrode with tip-plate structure is shown in Fig. 5a. The CNT film is grown on the tungsten tip cathode with 50 μm in diameter of the curvature, and is clipped in a stainless steel crack on the top of the stainless steel pole cathode. The stainless steel pole is fixed on the stainless plate cathode. The anode is a stainless plate, the gap is insulated

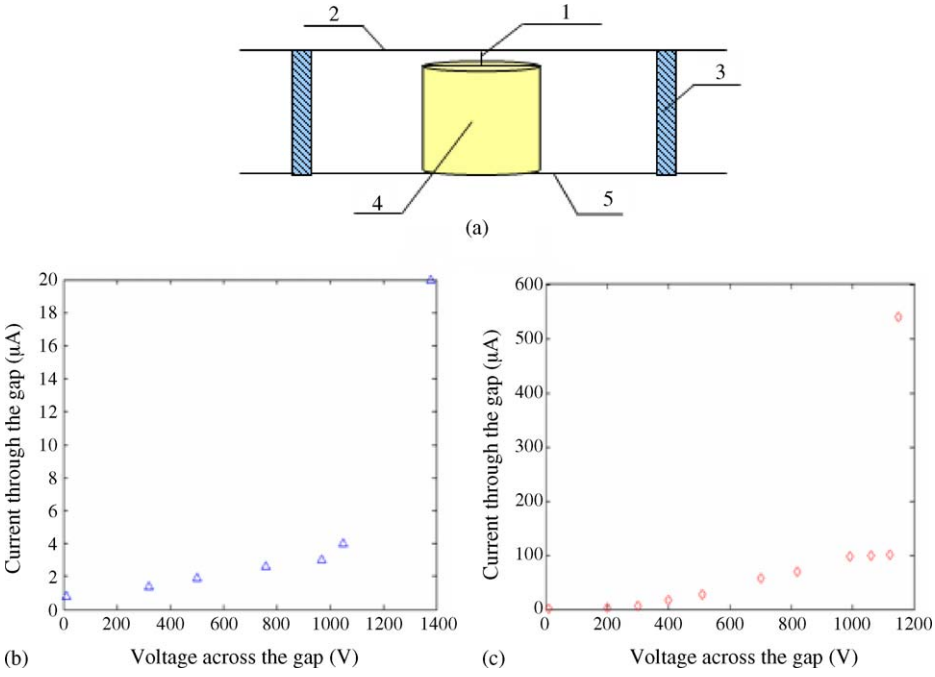

Fig. 5. #4 CNTFC tip-plate electrode. (a) The structure of #4 electrode (1, the tip cathode of W with the CNT film covering; 2, the stainless steel anode plate; 3, the polytetrafluoroethylene insulator; 4, the stainless steel pole cathode with the crack on the top; 5, the stainless steel plate cathode); (b) the discharge *I–V* characteristic of #4 electrode in air; (c) the discharge *I–V* characteristic of #4 electrode in CH_4–N_2 mixture at the CH_4 concentration $20{,}000 \times 10^{-6}$ L/L.

by the polytetrafluoroethylene, and the separation between the cathode and the anode is 100–170 μm.

4.4.2. Experimental study of discharge principle of #4 CNTFC electrode

#4 Tip-plate structure electrode with the gap distance 170 μm is used to conduct the experiments and study *I–V* characteristics. *I–V* characteristic of air is obtained and shown in Fig. 5b. *I–V* characteristic of CH_4–N_2 mixture at the concentration $20{,}000 \times 10^{-6}$ L/L of CH_4 component is obtained and shown in Fig. 5c. The corona discharges occur and the corona discharge voltages are very high. The breakdown voltage of #4 electrode in air is 1380 V and that at the concentration $20{,}000 \times 10^{-6}$ L/L of CH_4 component in CH_4–N_2 mixture is 1150 V. It shows that because the distribution of the electrode field is very nonuniform, the corona discharges occur and there are the light phenomena around the tungsten tip cathode covered with CNT film.

4.5. Design and study of #5 CNTFC electrode with strip-strip structure

4.5.1. Design of #5 CNTFC electrode with strip-strip structure

In comparison with #2 electrode, #5 electrode with strip-strip structure (Fig. 6) takes out the ITO film glass plate cathode, and only uses the strip of the CNT film as the cathode. The ITO film glass plate anode has two ventilating troughs with 0.3 cm width, and the effective face-to-face area between the cathode and the anode decreases to 0.15 cm × 0.3 cm (0.45 cm^2).

4.5.2. Experimental study of discharge principle of #5 CNTFC electrode

#5 CNTFC electrode with strip-strip structure has the corona discharge with the light phenomenon in air and CH_4–N_2 mixture, however the breakdown in the gap does not occur yet when the voltage between the cathode and the anode increases to 1200 V. Thus, the experiment study of the electrode stopped at once.

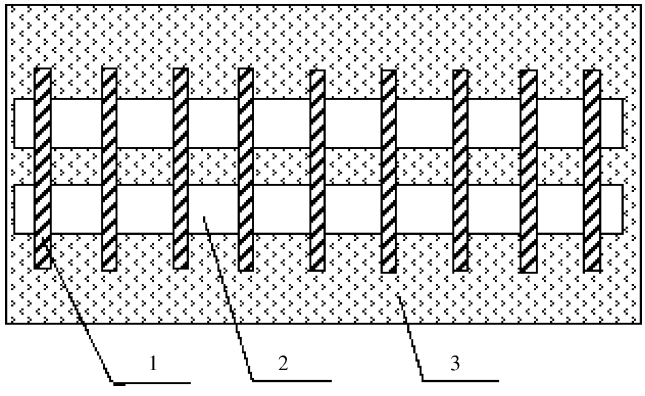

Fig. 6. #5 CNTFC strip-strip electrode with the ventilating trough (1, the CNT film cathode; 2, the ventilating trough; 3, ITO film conductance glass plate anode).

5. Simulation analysis of the electric field distribution in the gap of CNTFC

There have been many studies on the effect of the structures of CNT and CNT film on the electric field distribution, but they all aim at increasing the field electron emission current [31–33]. And because different structures of CNT and CNT film have different calculation results, the calculation results are not usable for different structures of CNT film cathodes. Thus, the electric field distributions in the gaps of the five CNTFCs are calculated and analyzed on the ANSYS software platform [34–36] based on the finite element method.

The structure of the CNTFC is very complex, and there is the nanometer structure of the carbon nanotubes as well as the millimeter structures of the cathode plate and the anode plate. Thus, if the whole field region of the CNTFC is divided into the elements with nanometer size, there will be large quantity of elements, and the computer resource will be not enough for the calculation of the field distribution on ANSYS software platform. If the whole field region of the CNTFC is divided into the elements with larger size than nanometer such as micrometer size, the quantity of elements will decrease, however the calculation deflection of the field intensity around the nanometer structure of the carbon nanotubes will be relatively large. So, the structure is divided into two parts for the accurate calculation of the field distribution of the whole field region: (1) the macrostructure: the micro structure of the CNTs is ignored and the effect of the ventilating holes and troughs on the electric field distribution is taken into account; (2) the microstructure: the electric field distribution of the microstructure around the CNTs is taken into account.

In considering the characteristic of the structure of #4 electrode, the electric field distribution of the macrostructure of #4 electrode could be approximated by that of the microstructure of a single carbon nanotube.

5.1. Calculation of the electric field distribution of the macrostructure

Taking #2 electrode for example, we will introduce the calculation of the electric field distribution of the macrostructure of the CNTFCs in the following.

5.1.1. Establishing the region of the macrostructure

The establishment procedure of the field region of the macrostructure of the CNTFC with #2 electrode is introduced as an example. Because of the limitation of the computer resource, the electric field region model of the macrostructure is one part of the actual model (Fig. 7a–c), shown in Fig. 7d. The area of the electric field region is chosen as 4.4 mm × 4.4 mm (19.36 mm^2), which is the hatched region in Fig. 7a and b. The separation between the cathode and the anode is 170 μm, the CNT film is 1.5 mm wide, 4.4 mm long and 0.50 mm thick, and the conductance glue is 0.50 mm thick. Thus, the thickness of the field region is 1.17 mm. The ventilating holes in the cathode plate and the anode plate are 4 mm in diameter, with 3 mm in separation between holes.

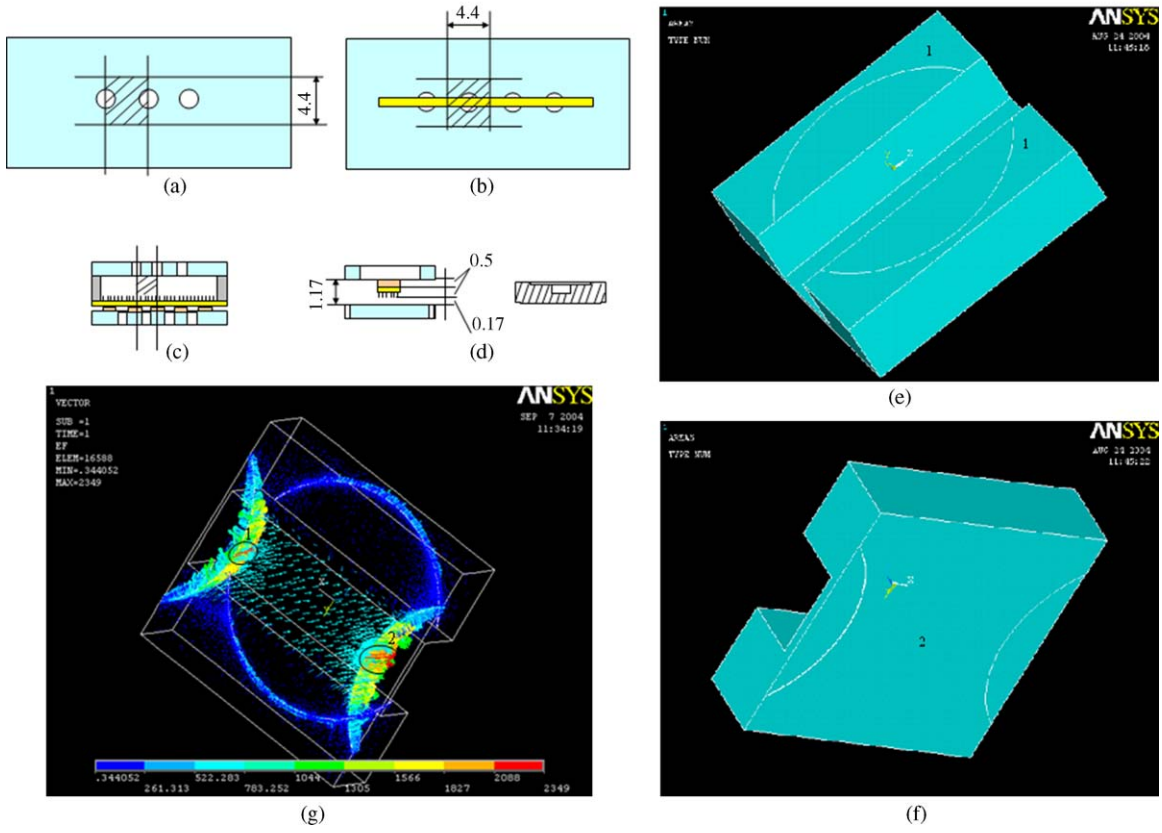

Fig. 7. The electric field region and the electric field distribution of the macrostructure of #2 strip-plate electrode with small holes. (a) The area of the electric field region of the macrostructure in the anode plate (the hatched region) with the datum unit—mm; (b) the area of the electric field region of the macrostructure in the cathode plate (the hatched region) with the datum unit—mm; (c) the area of the electric field region of the macrostructure between the anode and the cathode plates (the hatched region); (d) the section of the macrostructure region with the data unit—mm; (e) the downward view of the macrostructure of the field region of #2 CNTFC electrode; (f) the upward view of the macrostructure of the field region of #2 CNTFC electrode; (g) the electric field distribution of the macrostructure region of #2 CNTFC electrode.

Then, the field region is established on the ANSYS software platform and is 4.4 mm wide, 4.4 mm long, and 1.17 mm thick, shown in Fig. 7e and f. There are one ventilating hole of 0.01 mm in depth on the cathode surface of No. 1 shown in Fig. 7e and parts of two ventilating holes of 0.01 mm in depth on the anode surface of No. 2 shown in Fig. 7f. The three thin ventilating holes are all 4 mm in diameter and 3 mm in separation between holes. They are subtracted from the field region to simulate and analyze the effect of the ventilating holes on the field distribution.

5.1.2. Calculation and analysis of the electric field distribution of the macrostructure

The electric field distribution (Fig. 7g) of the macrostructure of #2 electrode in the field region is calculated on the ANSYS software platform and the finite element method. The ventilating holes in Fig. 7g are 4 mm in diameter, and the gap distance is 170 μm. The initial condition of the voltage across the gap is 100 V and the medium in the field region is air. In Fig. 7g, the sign of "MAX" is the maximum value E_{max} of the electric field intensity, and the regions in the two black circles of No. 1 and No. 2 have the higher electric field intensity. We can see that E_{max} of #2 electrode with the ventilating hoes of 4 mm in diameter is 2349 V/mm, viz. 2.349 V/μm. Then, the electric field distributions of the macrostructure of #2 electrodes with small ventilating holes (2 mm and 3 mm in diameter, respectively) are calculated, and so are other electrodes of #3 and #5. The gap distance and the initial voltage across the gap are the same as those of #2 electrode. The calculation results E_{max} of #2, #3, and #5 electrodes are shown in Table 3. According to the calculation results E_{max} in Table 3, the enhancement coefficients f could be calculated and are also shown in Table 3. $f = E_{max}/\bar{E}$, where $\bar{E}$ is the mean value of the electric field intensity. When $f > 4$, the electric field distribution is very nonuniform, the electric field near the cathode surface (viz. the local electric field) is very high, thus the gas near the cathode surface will have the local breakdown, viz. the corona discharge. When $f < 4$, the electric field distribution is relatively uniform, and the corona discharge is not easy to occur. It can be seen from Table 3 that:

(1) The enhancement coefficients of #2 CNTFC electrodes with small holes (2 mm, 3 mm, and 4 mm in diameter) are all less than 4, thus the corona discharge is not easy to occur. However, small ventilating holes are not favorable for the space charge to diffuse. Thus, #2 CNTFC electrode with the ventilating holes of 4 mm in diameter is superior to those with the ventilating holes of 2 mm and 3 mm in diameter.

Table 3
The calculation results of the macrostructures of #2, #3, and #5 electrodes

Electrode	Ventilating holes/trough size (mm)	E_{max} (V/μm)	f	Initial voltage across the gap (V)	$\bar{E}$ (V/μm)
#2	2 (hole)	2.276	3.8692		
	3 (hole)	2.279	3.8743		
#3	4 (hole)	2.349	3.9933	100	0.588235
	8 (cathode hole) and 10 (anode hole)	2.403	4.0851		
#5	3 (trough)	3.508	5.9636		

(2) The enhancement coefficients of #3 and #5 electrodes are more than 4, thus the corona discharge is easy to occur.
(3) For #2 CNTFC electrode with the ventilating holes of 4 mm in diameter, the electric field at the common boundary between the CNT film and the ventilating holes on the anode plate is much ($E_{max}/\bar{E} = 2.349/0.588235 = 3.9933$, viz. 2.9933 times) higher than that at the CNT film surface facing the area between the ventilating holes on the anode plate. The breakdown voltage of #2 electrode in air, with the ventilating holes of 4 mm in diameter and 170 μm in the gap distance, is 90 V, 2.6667 times less than that of #1 plate-plate electrode with the same gap distance in air, 330 V. It shows that the breakdown voltage could decrease the same times as the electric field increases, and the calculation result coincides with the experiment result.

Thus, it can be seen that the macrostructure of #2 CNTFC electrode with the ventilating holes of 4 mm in diameter is the most optimized among the five electrodes shown in Table 3.

5.2. Calculation of the electric field distribution of the microstructure

It is known that the electric field intensity is greatly high at the tip of a single CNT, however how much will be the electric field intensity of the CNT array? It is supposed for a long time that the electric field intensity of the CNT array would be very high because of the nanometer curvature of the CNT tip. If this does exist, the CNTFC will never have the self-sustaining dark discharge but the corona discharge with the light phenomenon. The supposition is in contradiction with the experiment phenomenon, thus the effect of the CNT number in the CNT array on the electric field intensity is simulated and studied in the following.

5.2.1. Calculation of the electric field distribution of three-dimensional (3-D) microstructure

(1) The calculation of the electric field of CNTFC with the gap distance of 170 μm: Approximate calculation of the relationship between the maximum electric field and the CNT number is conducted. The range of the CNT number is from 1 to 169. Note that, in comparison with the real electric field region with the gap distance of 170 μm, the size of the CNT (with 50 nm in diameter, 50 nm in separation between nanotubes and 4 μm in length) is greatly small, and the area of CNT array with tens to one hundred CNTs is also relatively small. Thus, there is also the problem of the limitation of the computer resource. Two methods were adopted to solve the problem: First, an approximation of the real field region was made in the following:
   (a) The length of the CNT, 4 μm, decreases 80 times to 50 nm.
   (b) The gap distance, 170 μm, decreases 80 times to 2125 nm.
   (c) The area of the field region is 2 μm × 2 μm (4 μm^2).

   Second, a nonuniform meshing was conducted in the following:
   (a) The meshing with small element in nanometer order was conducted near the nanotubes.
   (b) The meshing with large element in micrometer order was conducted in the other parts of the field region.

   The schematic micro-region of the microstructure of the CNTFC electrode is shown in Fig. 8a and b, and the 3-D region of the micro-region with 81-CNT array is established, shown in Fig. 8c. In condition of the initial voltage across the gap 100 V and the medium in the field region being air, the maximum electric field intensity and the electric field enhancement coefficient at different CNT number with the range of 1–169 are calculated and listed in Table 4.
(2) The calculation of the electric field of CNTFC with the gap distance of 100 μm: The similar approximate micro-region of the CNTFC with the gap distance of 100 μm was also made in the following:
   (a) The length 4 μm of the CNT and the gap distance 100 μm decrease the same (80) times to 50 nm and 1250 nm, respectively.

Table 4
The three-dimensional calculation results of the effect of the CNT number on the electric field distribution (the CNTFC electrodes with the gap distances 100 μm and 170 μm)

CNT number	170 μm		100 μm	
	E_{max} (V/nm)	f	E_{max} (V/nm)	f
1	0.248221	5.275	0.408811	5.110
9	0.182061	3.869	0.350994	4.387
25	0.14983	3.184	0.366453	4.581
49	0.119932	2.549	0.277499	3.469
81	0.11633	2.472	0.325183	4.065
121	0.134452	2.857	0.278052	3.476
169	0.137704	2.926	0.265815	3.323

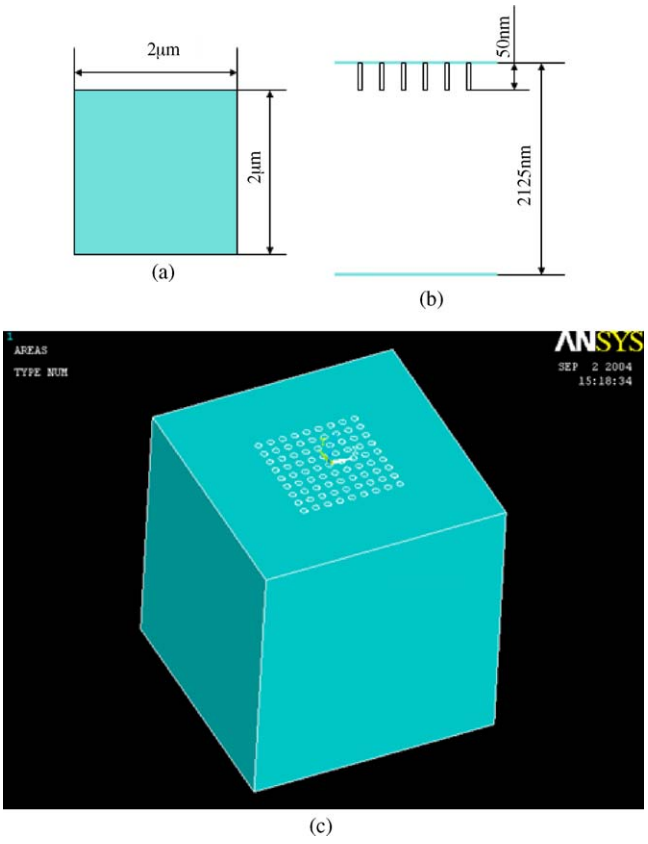

Fig. 8. The microstructure of the CNTFC electrode. (a) The area of the microstructure region; (b) the section of the microstructure region; (c) the microstructure region with 81-CNT array.

(b) The area of the field region is 2 μm × 2 μm (4 μm^2).

In condition of the initial voltage across the gap 100 V and the medium in the field region being air, the maximum electric field intensity and the electric field enhancement coefficient at different CNT number with the range of 1–169 are calculated and listed in Table 4.

(3) Analysis of the electric field distribution of the two approximate micro-regions: The above calculations of the two micro-regions show that:
   (a) The electric field of a single CNT cathode is greatly high, and the electric field distribution is very nonuniform, thus the corona discharge is very easy to occur. The calculation result could explain the experiment result of #4 CNTFC electrode with tip-plate structure.
   (b) When the nanotube number increases, the maximum electric field intensities of the CNTFCs with two different gap distances (170 μm and 100 μm) decrease and the electric field distributions are getting more uniform.
   (c) When the nanotube number increases, the change of the maximum electric field intensity is getting smaller. Thus, the electric field distribution of the CNT film with large area in macroscopy could be approximate with that of several-tens-CNT array.

From the calculation result of the microstructure, it can be seen that although the electric field distribution of a single CNT is greatly nonuniform, that of the CNT array is getting more uniform when the CNT number increases, and the corona discharge is not easier to occur.

5.2.2. Calculation of two-dimensional (2-D) microstructure

Calculation of 2-D microstructure needs less computer resource, thus the real region of the CNTFC electrode could be calculated approximately. The calculation condition is as the following:

(a) The separations between the cathode and the anode are 100 μm and 170 μm, respectively.
(b) The areas of the cathode and the anode plates are all 1 mm × 1 mm (1 mm^2).
(c) The CNT is 50 nm in diameter, 4000 nm long and 50 nm in separation between nanotubes.
(d) The initial voltages between the cathode and the anode are 100 V and 200 V, respectively.

Because of the large 2-D electric field region and the limitation of the computer resource, the CNT number in calculation of 2-D microstructure is less than that in calculation of 3-D microstructure. The calculation results of the effect of the CNT number on the maximum electric field intensity are shown in Fig. 9a and b. The conclusion same as that of the 3-D calculation is obtained: the electric field intensity of a single CNT is greatly nonuniform, however that of the CNT array is getting more uniform when the CNT number increases.

5.2.3. Integrated analysis of the electric field distribution of the macrostructure and the microstructure

When the enhancement coefficient f is more than 4, the electric field distribution is very nonuniform. The CNTFC has the corona discharge, and the breakdown voltage is high.

When f is less than 4, the electric field distribution is relatively uniform. The CNTFC has the self-sustaining dark discharge, and the breakdown voltage is low. The maximum electric field intensity at the common boundary between the CNT film and the ventilating holes on the anode plate is much higher than that at the CNT film surface facing the area between the ventilating holes on the anode plate. The breakdown voltage decreases much when $f > 2$ and the gap distance is in micrometer order, in comparison with that of #1 electrode with the relatively uniform electric field distribution. Thus, the ventilating holes not only make the space charge in the gap convenient to diffuse, but also make the breakdown voltage decreasing.

It shows that the structure of #2 CNTFC electrode is the best optimized among the five electrodes of #l–5, and could be used to fabricate a gas sensor and measure gas.

5.3. Effect of different gap distances on the electric field distribution

The effect of different gap distances on the electric field distribution was also studied in an approximate micro-region,

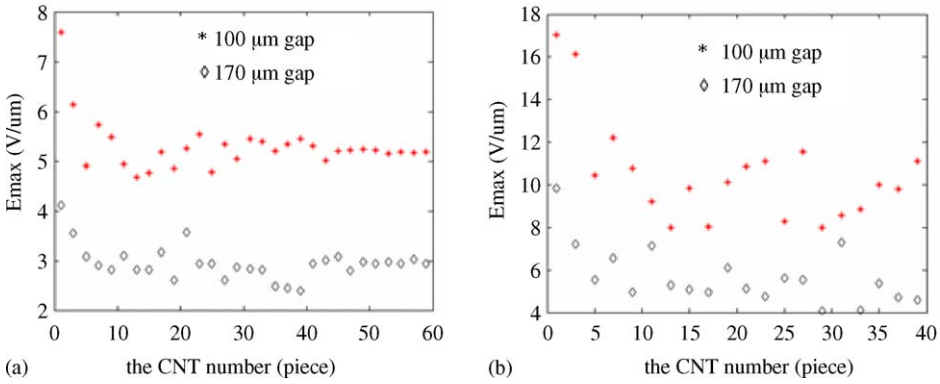

Fig. 9. Two-dimensional calculation results of the effect of the CNT number on the maximum electric field intensity E_{max}. (a) The effect of the CNT number on the maximum electric field intensity E_{max} of the CNTFC electrodes with the gap distances 100 μm and 170 μm, respectively, at the initial voltage across the gap 100 V; (b) the effect of the CNT number on the maximum electric field intensity E_{max} of the CNTFC electrodes with the gap distances 100 μm and 170 μm, respectively, at the initial voltage across the gap 200 V.

Table 5
The calculation results of the effect of different gap distances on the electric field distribution

Sequence number	Gap distance (nm)	E_{max} (V/nm)	$\bar{E}$ (V/nm)	f
1	10	16.5700	10.0000	1.6570
2	30	8.5950	3.3333	2.5785
3	50	4.2730	2.0000	2.1365
4	70	3.2500	1.4286	2.2750
5	150	1.7480	0.6667	2.6220
6	450	0.5820	0.2222	2.6190
7	950	0.3070	0.1053	2.9165
8	4950	0.0487	0.0202	2.4107
9	9950	0.0270	0.0101	2.6865

similar with those in the parts of (1) and (2) in Section 5.2.1. The approximation was made in the following:

(1) The CNT is 50 nm in diameter and 50 nm in separation between nanotubes, 50 nm in length.
(2) There are 25-CNTs in the CNT array.
(3) The effective face-to-face area between the cathode and the anode is 1 μm × 1 μm = (1 μm^2).

The electric field distributions of the microstructures of the CNTFCs with different gap distances are calculated, and the electric field enhancement coefficients are calculated and shown in Table 5.

It shows that in condition of the CNT with 50 nm in length and 25-CNT array in the approximate micro-region, the electric field enhancement coefficients are less than 4 in the range of the gap distance 10–10,000 nm. The length of CNT 50 nm and the gap distance 10–10,000 nm are amplified 80 times, same as that in establishing the micro-region. And then the real gap distance range of CNT with 4 μm in length is 0.8–800 μm. Thus, the self-sustaining discharge will occur in the very large range of the gap distance of 0.8–800 μm of the CNTFC.

6. Conclusion

(1) The CNT film is used as the cathode to fabricate the electrode. The breakdown voltages of the CNT film cathode decrease from the value of more than thousand volts of the traditional discharge gas sensor to several hundred volts, in the gap distance with micrometer order at the atmospheric pressure. The current at the breakdown is microampere order, increasing three orders in comparison with that of the novel MEMS discharge gas sensor in reference [26].
(2) The experiment studies of the five electrode structures are conducted. It shows that #2 electrode has the best performance, such as the low working voltage, the space charge in the gap easy to diffuse, and no light phenomenon during discharge. Thus, #2 electrode could be used as a gas sensor.
(3) The effects of the five CNTFC electrode structures on the electric field distribution are studied on the ANSYS software platform and the finite element method, and the electric field enhancement coefficients f are calculated. The electrode structure with $f < 4$ and the space charge in the gap easy to diffuse will have the self-sustaining dark discharge and could be used as a gas sensor. #2 Electrode has the ventilating holes and the calculation result of f is less than 4. The results of the simulations and the experiments show that it is reasonable to use #2 CNTFC electrode with low working voltage, self-sustaining dark discharge and the space charge in the gap easy to diffuse as a novel gas sensor.
(4) The calculation results of the electric field distribution of the CNTFC with different gap distances show that the electric field enhancement coefficients are less than 4 in the range of the gap distance 0.8–800 μm in condition of the CNT with 50 nm in diameter and 4 μm long. The self-sustaining dark discharge will occur in the very large range of the gap distance of the CNTFC gas sensor. Thus, it is possible to fabricate CNTFC gas sensor array with n CNTFC gas sensors in different gap distances to measure gas mixture with n components.

Acknowledgements

The authors would like to thank the National Nature Science Foundation Committee of China. This subject is supported by the National Nature Science Foundation of China (50077016), (60276037) and (60036010), and also by the National Study

and Development Plan Subject on High Technology of China (2001AA313090).

References

[1] H. Endres, R. Hartinger, M. Schwaiger, G. Gmelch, M. Roth, A capacitive CO_2 sensor system with suppression of the humidity interference, Sens. Actuators B 57 (1999) 83–87.
[2] M. Lee, J. Meyer, A new process for fabricating CO_2 sensing layers based on $BaTiO_3$ and additives, Sens. Actuators B 68 (2000) 293–299.
[3] S. Matsubara, et al., A practical capacitive type CO_2 sensor using CeO_2/$BaCO_3$/CuO ceramics, Sens. Actuators B 65 (2000) 128–132.
[4] J. Carrie, A. Essalik, J. Marusic, Micromachined thin film solid state electrochemical CO_2, NO_2 and SO_2 gas sensors, Sens. Actuators B 59 (1999) 235–241.
[5] M. Longergan, et al., Array-based vapor sensing using chemically sensitive, carbon black-polymer resistors, Chem. Mater. (8) (1996) 2298–2312.
[6] M. Dresselhaus, G. Dresselhaus, P. Avouris, Carbon nanotubes—synthesis, structure, properties and applications, Top. Appl. Phys. 80 (2001) 391–425.
[7] R.H. Baughman, A.A. Zakhidov, De Heer, A. Walt, Carbon nanotubes—the route toward applications, Science 297 (2002) 787–792.
[8] The Environmental Response Team Standard Operating Procedure No. 2114, Environmental Protection Agency, Washington, DC, 1994. ⟨http://www.dem.ri.gov/pubs/sops/wmsr2114.pdf⟩.
[9] Flame ionization detector, product data sheet, SRI Instruments, Torrance, CA, 1998. ⟨http://www.srigc.com/FID.pdf⟩.
[10] R. Kocache, Gas sensor (toturiels), Sens. Rev. 14 (1) (1994) 8-1(-6).
[11] S. Matsuura, New development and applications of gas sensors in Japan, Sens. Actuators B 13 (1993) 1–3, 7–11.
[12] H. Wuo, K.M. Lee, C.C. Liu, Development of chemicalsensors using micro fabrication and micromachine techniques [J], Sens. Actuators B 13 (1993) 2–5.
[13] J.J. Ho, Y.K. Fang, High sensitivity ethanol gas sensor integrated with a solid-state heater and thermal isolation improvement structure for legal drink–drive detecting [J], Sens. Actuators B 50 (1998) 225–232.
[14] P. Pasierb, S. Komornicki, R. Gajerski, Electrochemical gas sensor materials studied by impedance spectroscopy [J], J. Electrocerm. 8 (1) (2002) 57–64.
[15] S. Quah, K. Danowski, P. Pantano, Therapeutic micro and nanotechnology Section: microwell array photoimprint lithography: micropost sensors and guidance of PC 12 neurite processes [J], Biomed. Microdevices 4 (3) (2002) 123–130.
[16] T. Maekwa, et al., Sensing behavior of CuO-Loaded SnO_2 element for H_2S detection, Chem. Lett. (1991) 575.
[17] H. Zwahara, et al., Hydrogen and steam sensors using $BaCeO_3$ based proton-conducting ceramics operative at 200–900 °C, Electrochem. Soc. 138 (1991) 98.
[18] N. Yamazoe, et al., Solid-state glucose sensor using LaF_3-based transducer, Jpn. J. Appl. Phys. 30 (1991) 1954.
[19] T. Ishihara, et al., Application of mixed oxide capacitor to the selective carbon dioxide sensor, J. Electro. Chem. Soc. 138 (1991) 173.
[20] T. Nakahar, H. Kada, Tin dioxide gas sensor—a new approach to order sensing, Chem. Sens. Technol. (3) (1991) 19.
[21] S.M. Klainer, Environmental applications of fiber opticchemical sensors [J], Opt. Chem. Sens. 28 (6) (1991) 83–96.
[22] P. Collins, K. Bradley, M. Ishigami, A. Zettl, Extreme oxygen sensitivity of electronic properties of carbon nanotubes, Science 287 (2000) 1801–1804.
[23] J. Kong, et al., Nanotube molecular wires as chemical sensors, Science 287 (2000) 622–625.
[24] W. Jin, G. Stewarr, B. Culshaw, Source noise limitation in a fiber optics gas sensors using a broadband source [J], Appl. Opt. 35 (5) (1994) 55–62.
[25] Y.T. Wang, Z. Meng, W.D. Liu, Environmental monitoring with optica fibre gas sensor [J], World Sci.-tech. R&D 23 (6) (2001) 19–21.
[26] P.H. Dai, B.M. Ling, Study of anew gas sensor based on electrical conductance of gases in a high electrical field, China Instrum. Control Soc. 19 (3) (1998) 239–244.
[27] Y. Zhang, J.H. Liu, W.H. Liu, J.Y. Dou, Y.N. He, Study of gas sensor with carbon nanotube film on the substrate of porous silicon, in: IEEE 14th International Vacuum Microelectronics Conference Proceedings, Boston, USA, 2001, pp. 13–14.
[28] A. Modi, N. Koratkar, E. Lass, B.Q. Wei, P.M. Ajayan, Miniaturized gas ionization sensors using carbon nanotubes, Nature 24 (July (10)) (2003) 171–174.
[29] X. Li, et al., Study of catalyst grains effect on self-sustaining discharge carbon nanotubes gas sensor array, China Instrum. Control Soc. 24 (1) (2003) 49–52.
[30] X. Li, et al., Study of catalyst grains effect on electrode of self-sustaining discharge carbon nano-tubes gas sensor array, in: IEEE 14th International Vacuum Microelectronics Conference Proceedings, Boston, USA, 2001, pp. 65–66.
[31] W. Rust, K. Schweizerhof, Finite element limit load analysis of thin-walled structures by ANSYS (implicit), LS-DYNA (explicit) and in combination, Thin-Walled Struct. 41 (February (2–3)) (2003) 227–244.
[32] M.A. Feltus, U. Shoop, TRAC-BF1 three-dimensional BWR vessel thermal-hydraulic and ANSYS stress analyses for BWR core shroud cracking, Ann. Nucl. Energy 25 (January (1–3)) (1998) 65–81.
[33] V. Manet, The use of ANSYS to calculate the behaviour of sandwich structures, Compos. Sci. Technol. 58 (12) (1998) 1899–1905.
[34] A.L. Musatov, et al., Field electron emission from nanotube carbon layers grown by CVD process., Appl. Surf. Sci. 183 (2001) 111–119.
[35] F.H. Read, N.J. Bowring, Field enhancement factors of random arrays of carbon nanotubes, Nucl. Instrum. Methods Phys. Res. 519 (2004) 305–314.
[36] V. Filip, et al., Modeling the electron field emission from carbon nanotube films, Ultramicroscopy 89 (October) (2001) 39–49.

Biography

Zhang Yong is an associate-professor with Xi'an Jiaotong University, China, where she received her doctor degree in 2004. Her interests are nanometer sensor system, intelligent sensor system, modern measurement and control instruments, multi-information fusion technology of multi-sensors, signal processing, and integrated virtual instruments.